AUT Journal of Civil Engineering

AUT J. Civil Eng., 4(1) (2020) 37-54
DOI: 10.22060/ajce.2019.15026.5517

Developing three hybrid machine learning algorithms for predicting the mechanical properties of plastic concrete samples with different geometries

A. Tavana Amlashi[1*], A.R. Ghanizadeh[2], H. Abbaslou[2], P. Alidoust[3]

[1]Young Researchers and Elite Club, Rasht Branch, Islamic Azad University, Rasht, Iran
[2]Department of Civil Engineering, Sirjan University of Technology, Sirjan, Iran
[3]Department of Civil Engineering, Iran University of Science & Technology, Tehran, Iran

ABSTRACT: Plastic concrete is an engineering material, which is commonly used for construction of cut-off walls to prevent water seepage under the dam. This type of concrete shows great promise to satisfy the requirements of the strength, stiffness and permeability for remedial cut-off wall construction. This paper aims to explore three hybrid machine learning algorithms including Artificial Neural Network (ANN), Support Vector Machine (SVM) and Adaptive Neuro-Fuzzy Inference System (ANFIS) optimized with Particle Swarm Optimization (PSO) to predict the compressive and splitting tensile strength of plastic concretes. To this end, data were collected from different sources and data gaps were covered by extra experimental tests and finally, 387 data for compressive strength and 107 data for splitting tensile strength were gathered for modeling. This study shows that ANN-PSO is superior to SVM-PSO and ANFIS-PSO in case of predicting compressive as well as splitting tensile strength of plastic concretes. The coefficient of determination (R2) in case of ANN-PSO for both training and testing sets is more than 0.95. Results of this study can be used to predict the compressive and splitting tensile strength of plastic concretes with regards to constituent materials and specimen geometry of plastic concrete.

Review History:

Received: 2018-09-24
Revised: 2019-03-10
Accepted: 2019-03-15
Available Online: 2019-03-15

Keywords:

plastic concrete
compressive strength
splitting tensile strength
machine learning algorithms
particle swarm optimization

1. INTRODUCTION

Water tightness and seepage control are important considerations in the design and construction of dams. Various methods exist to prevent the seepage of water from dams. In this regard, the construction of cut-off walls is one of the most common ways to prevent water seepage under a dam. Based on the rigid diaphragm of cut-off walls in their simplest structural form, any deformation of earth embankment may lead to its rupture. The importance of rupture considerations greatly returns to decreasing flow efficiency of the cut-off walls and consequently compromising the safety of dams. On the other hand, deformations of earth embankments due to fluctuations in impounded reservoir level or seismic activity can cause to develop cracks in concrete cut-off wall [1]. As a solution for this issue, engineers have used plastic concrete with similar deformation characteristics to dam embankment soils [2]. Plastic concrete consists of aggregate, cement, water, and bentonite clay which mixed at a high water cement ratio to produce a ductile material than conventional structural concrete [3]. It is worth noting that bentonite has so far, been defined and used for sealing purposes in civil and hydraulic engineering for a long period of time [4-12]. Plastic concrete must be strong and watertight and have stiffness comparable to the surrounding soil. Satisfying strain-compatibility between the wall and surrounding soil will moderate the likelihood of overstressing the wall and will allow the wall and soil to deform without separating [13]. This type of concrete shows great promise to satisfy the requirements of the strength, stiffness and permeability for remedial cut-off wall construction [14]. It has a higher formability, but lower strength and permeability that result from the usage of clay slurry in the concrete mix design [3]. Due to the importance of mechanical properties of plastic concrete and its direct impact on the quality of the cut-off walls implementation, numerous laboratory studies have been allocated to it by researchers[15-20].

Compressive and splitting tensile strength are two important parameters for quality control of concretes. Several factors can affect the compressive as well as tensile strength of plastic concretes including properties of concrete materials, mixing ratio, curing time and geometry of samples. Usually at the site of dam construction and during production of plastic concrete, samples taken from various mixers should be tested by specialized equipments and expert personnel and this is of a great importance. But due to special circumstances in workplace such as construction problems, storage and curing process of a large number of concrete samples and the necessity of faster awareness of the sample's resistance in order to amend the used ratios make this process encounter with

*Corresponding author's email: amir.tavana.amlashi@gmail.com

difficulties and clearly require more time and significant cost. Therefore, a relatively accurate and comprehensive estimate (in the desired confidence level) of compressive strength and tensile strength of concrete provides the needed tool for a correct decision.

In recent decades, various methods of data mining in civil engineering, especially in predicting the compressive and splitting tensile strength of different types of concrete, have attracted the attention of many researcher [21-23]. At the beginning of the use of data mining, machine learning methods, such as neural network prediction models, were preferred. This preference can be attributed to no need of neural networks for a predetermined mathematical model for their computations and tolerating experimental noise (inaccuracies) far better than other predicting methods [24]. However, as time passed other methods such as Fuzzy Polynomial Neural Networks (FPNN), Probabilistic Neural Networks (PNN), Adaptive Probabilistic Neural Network (APNN) and GMDH-type Neural Network were developed to increase the accuracy, speed and improving the performance of neural networks [25-29], but until now the largest share of literatures are allocated to artificial neural network method [30-36]. In addition to ANN, many researchers have used other machine learning methods, such as support vector machine (SVM) and adaptive neuro-fuzzy inference system (ANFIS), in their comparative researches[37, 38]. However, the SVM and ANFIS previously were used individually in many researches, and their high potential in the process of prediction has been approved in the past [39, 40]. Sobhani et al. (2013) compared ANN method with an optimized SVM to predict the compressive strength of no-slump concrete. The results showed the superiority of SVM modeling in terms of optimization speed in comparison with ANN method [38]. Also, Motamedi et al. (2015) worked on an ANFIS computing technique to predict the unconfined compressive strength of the pulverized fuel ash-cement-sand mixture. The analysis was based on countering the uncertainties in the system. In such circumstances, the results confirmed the ability of ANFIS method [41]. On the other hand, hybrid methods can be considered as a combination of ANN, SVM and ANFIS with evolutionary search procedures or optimization algorithms. Hybrid methods with optimization algorithms play an important role in purpose of identification the defects in the structure and compressive and splitting tensile strength of concrete [42-45].

Besides several research works in the field of prediction of compressive and splitting tensile strength of different types of concretes by using of machine learning methods, still lack of a research based on machine learning methods, in which the properties of plastic concrete is assessed is observable. In this paper, after the establishment of a comprehensive database for compressive and tensile strength of plastic concrete, three methods of ANN, SVM and ANFIS have been optimized in accordance with PSO algorithm to predict the compressive and splitting tensile strength of plastic concrete and finally their accuracy will be compared with respect to the training and testing sets.

2. MATERIALS AND METHODS

Among many machine learning methods for predicting numeric values that described in literature, it is still unclear which method has the best predicting performance. Performance of each method is dependent on the application area and can be changed by it [46]. In this study, the prediction of compressive and splitting tensile strength of plastic concrete were evaluated based on three hybrid machine learning methods including hybrid ANN-PSO, SVM-PSO, and ANFIS-PSO .

2.1. Particle Swarm Optimization

Flocking behavior of birds is the inspiration of an iterative computational method with worldwide reputation in numerical optimization problems which is known as particle swarm optimization (PSO)[47]. Popularity of this method originates from its efficiency and tractability in gradient free optimization algorithms especially on problems in which the gradient is too challenging, computationally expensive, or even impossible to derive. The procedure of optimizing starts by leading a randomly initialized population of candidate solutions (particles) around the problem's search-space. Position and velocity are key features of a particle that actually is being defined by them. According to the algorithm iterations, this model is expected, not guaranteed, to end up with global near-optima solution with a reasonable degree of accuracy. The behavior of particles is shown mathematically in the following equations:

$$v_i(t+1) = w(t)v_i(t) + \phi_1(t)(pbest_i(t) - x_i(t)) + \phi_2(t)(gbest\ (t) - x_i(t)). \tag{1}$$

$$\varphi_1(t) = c_1 r_1, \quad \varphi_2(t) = c_2 r_2(t) \tag{2}$$

$$x_i(t+1) = x_i(t) + v_i(t+1) \tag{3}$$

where $x_i(t)$ represents the position vector of the i th particle at time t, and $v_i(t)$ is its corresponding velocity vector. $pbest_i$ is the previous best known position of the i th particle and $gbest$ designates the entire swarm or each particle neighbor's best known position. c_1 and c_2 are the acceleration parameters, and r_1 and r_2 are random numbers regenerated in each iteration with uniform distribution ranged in [0, 1]. Besides, w that is known as the inertia coefficient indicates the particle momentum in its present direction, and defines the trade-off between exploration and convergence speed. As can be seen in Eq. (3), after the calculation of velocity for each particle the position is being updated. During the iteration process, the range of permissible velocities are usually being restricted and dampened due to obtaining a better exploration and eliminating the fluctuations caused by large velocities.

2.2. Artificial Neural Network (ANN)

The simulation of important features of the human nervous system is being used in a modeling tool that is known as Artificial Neural Network (ANN). It is notable that the past experiences play substantial rule in solving the problems by this method. Analogous to a human brain, an ANN uses many simple computational elements, named artificial neurons, connected by variable weights [48]. An artificial neuron is shown in Fig. 1. By training the ANN, reaching to a specific target with a particular input is being possible. The comparison of the output and the target enables this method to be trained and this will continue until the ANN output matches the target. Several pairs of inputs and targets are needed to train an ANN efficiently.

One kind of ANN method that is helpful in solving special problems with requirements like recognition of complex patterns and performing nontrivial mapping function is the feed-forward back-propagation neural network architecture that can be seen in Fig. 2 [49].

The training of aforementioned algorithm involves two steps [50, 51]:

· Forward Phase. During this phase, the free parameters of the network are being fixed. The propagation of input signal take place through the network layer by layer. This phase ends up with the computation of an error signal.

$$e_i = d_i - y_i. \tag{4}$$

Where d_i is the desired response, and y_i is the actual output produced by the network in response to the input x_i.

· Backward Phase. The backward direction for propagation of the error signal e through the network during this phase is the reason of this algorithm's name. During this phase, the error e is being minimized in a statistical by applying adjustments to the free parameters of the network.

Other method for training a neural network is meta-heuristic optimization method. In this technique weight and bias parameters of Artificial Neural Network are determined in such a way which RMSE of the observed and predicted values by using artificial neural network is minimized. In this research in order to determining the optimal amount of weight and bias parameters, the PSO algorithm was applied. Hybrid ANN-PSO flowchart is shown in Fig. 3.

2.3. Support vector machine (SVM)

The support vector machine (SVM) technique was first presented by Vapnik [52]. Due to reducing the upper bound generalization error in comparison with local training error, developments based on statistical machine learning development and structural risk minimization was applied to it. It is a common technique previously used in machine learning methodologies [53].

The SVM method has several advantages compared to other soft computing learning algorithms which are as follows: (1) by applying a high dimensional spaced set of kernel equations, which discreetly include non-linear transformation, makes linearly separable data indispensable and no need to assumption of functional transformation; and (2) The convex nature of the optimal problem makes this technique unique.

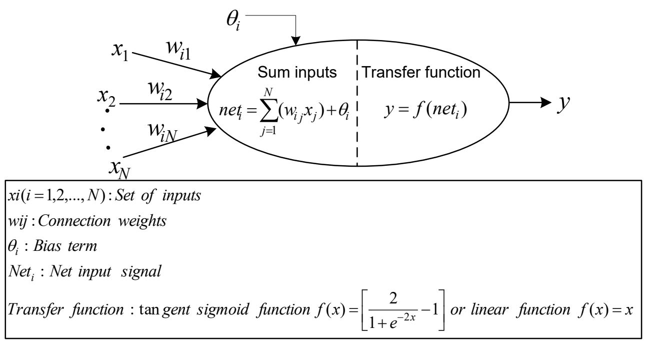

Fig. 1. Summation and transfer function of a typical artificial neuron.

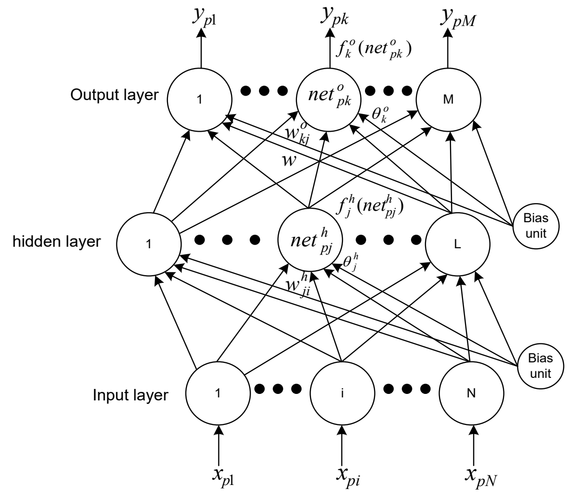

Fig.2. A feed-forward back-propagation network architecture with one hidden layer.

Eq. (5) to (8), represent the SVM functions in accordance with Vapnik's theory. $R = \{x_i - d_i\}_i^n$ is used to assume a set of data points, where x_i indicates the input space vector of the data sample and d_i is indicative of the target value and n is data size. The equations according to SVM estimates are as follow:

$$f(x) = w\varphi(x) - b. \tag{5}$$

$$R_{SVMs}(C) = \frac{1}{2}\|w\|^2 + C\frac{1}{n}\sum_{i=1}^{n} L(x_i, d_i) \tag{6}$$

Where $\phi(x)$ indicates the high dimensional space characteristic that maps the input space vector x while w and b are a normal vector and scalar, respectively.

In addition, $C\frac{1}{n}\sum_{i=1}^{n} L(x_i, d_i)$ stands for the empirical error, risk. Factors b and w are measured by minimizing a regularized risk equation followed by the introduction of positive slack variables ξ_i and ξ_i^* that indicate the upper and lower excess

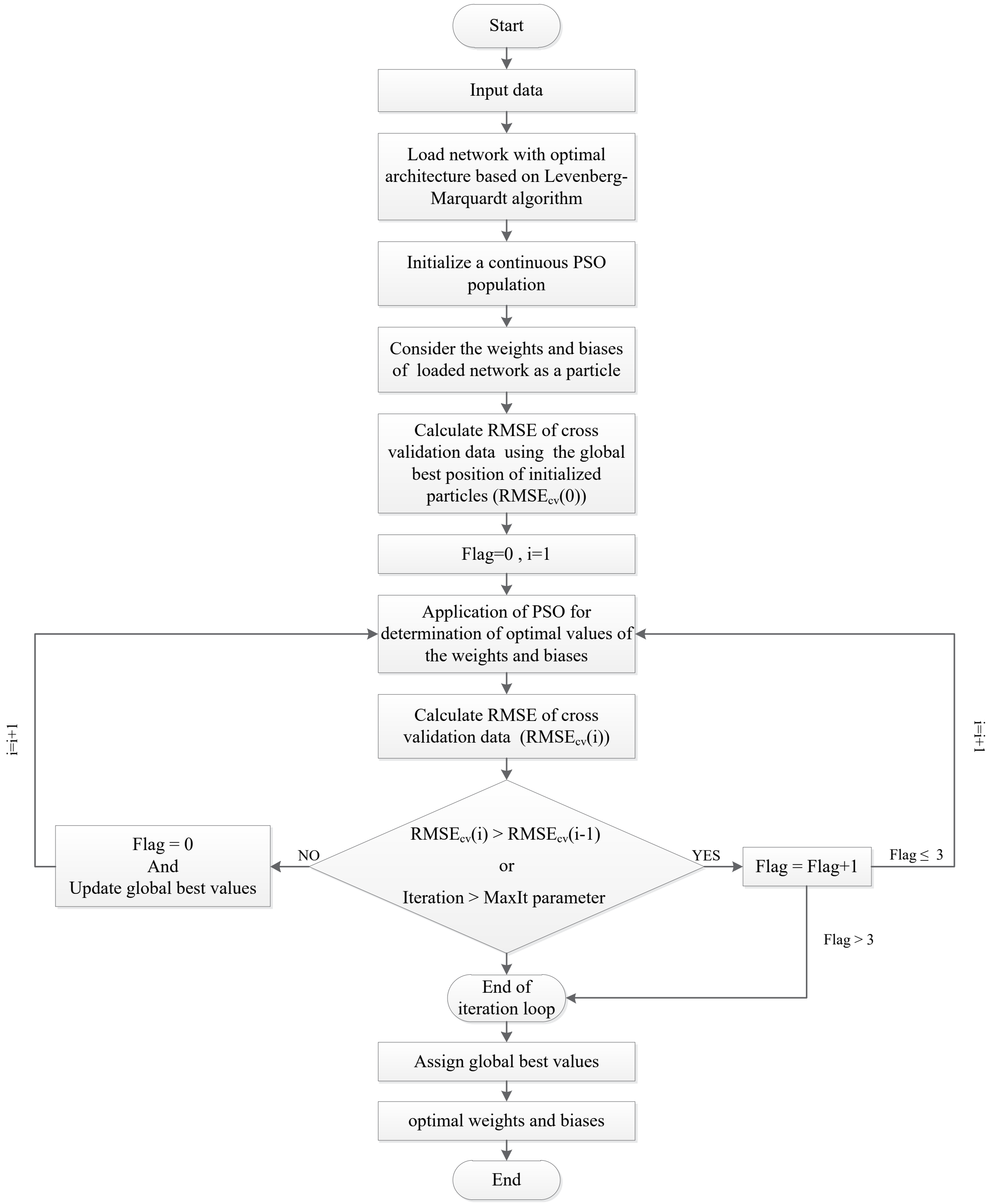

Fig. 3. Flowchart of ANN-PSO.

deviation (Wu and Wang, 2009):

$$Minimize\ \ R_{SVMs}(w,\ \xi^{(*)}) = \frac{1}{2}\|w\|^2 + C\frac{1}{n}\sum_{i=1}^{n} L(\xi_i,\ \xi_i^*). \tag{7}$$

$$\text{Subject to} \begin{cases} d_i = w\varphi(x_i) + b_i \leq \varepsilon + \xi_i \\ w\varphi(x_i) + b_i - d_i \leq \varepsilon + \xi_i^* \\ \xi_i, \xi_i^* \geq 0,\ i = 1 \ldots, l \end{cases}$$

where $\frac{1}{2}\|w\|^2$ is the regularization term, C represents the error penalty feature utilized to control the trade-off between the empirical error (risk) and regularization term, ε represents the loss function associated with the approximation accuracy of the trained data point, and the number of factors in the training data set is defined as l.

The following generic function is being used to obtain optimality constraints and the Lagrange multiplier that are the requirements of solving Eq. (8):

$$f(x, a, a_i^*) = \sum_{i=1}^{n}(a_i - a_i^*)K(x, x_i) + b. \tag{8}$$

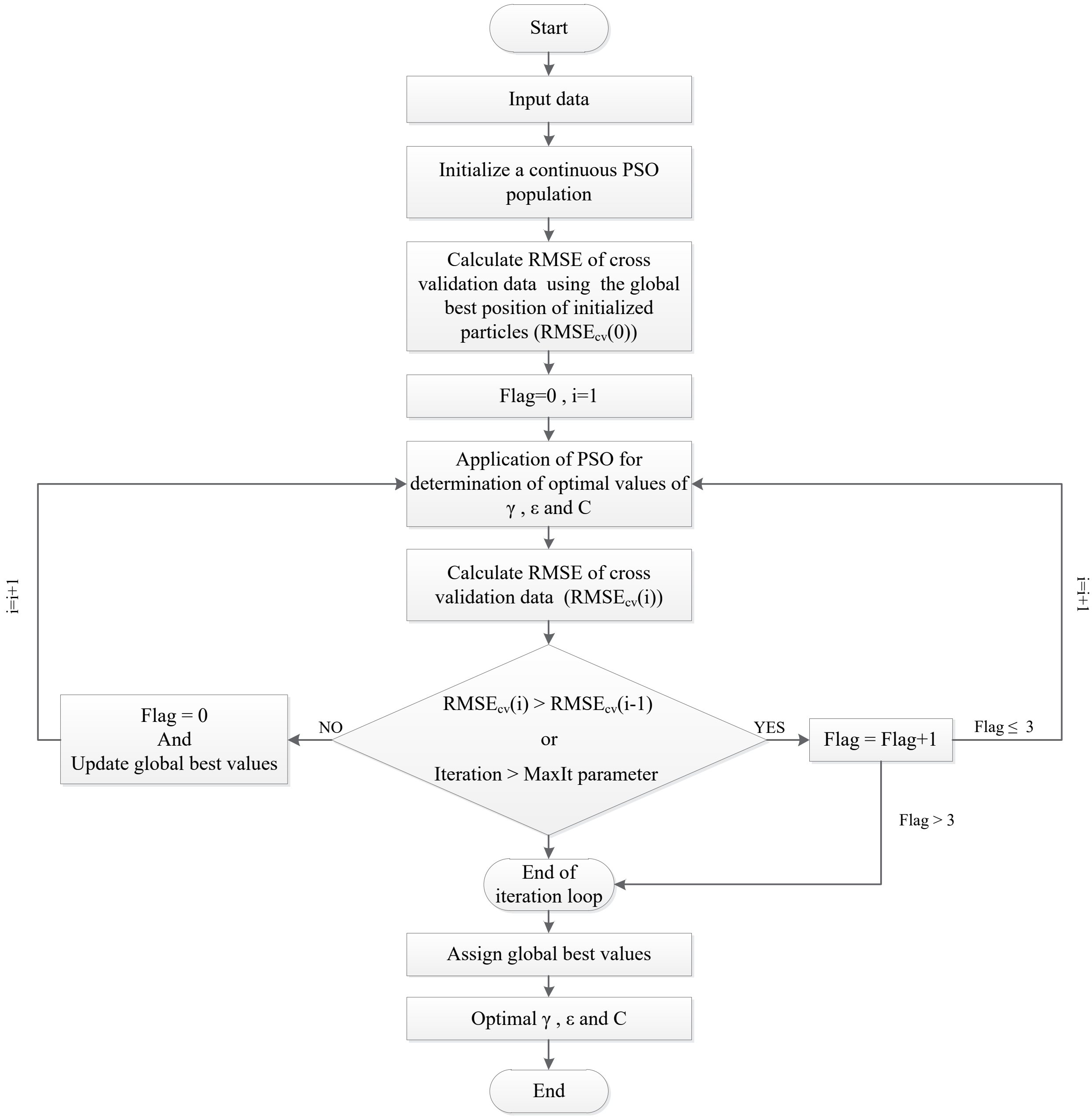

Fig. 4. Flowchart of SVM-PSO.

$K(x, x_i) = \varphi(x_i)\varphi(\dot{x})$ in Eq. (8), refers to the kernel function, which is dependent on the two inner vector x_i and x_j in the feature space $\varphi(x_i)$ and $\varphi(xj)$, respectively. In this study, Radial Bias Function (RBF), was considered as kernel function which is defined as follows:

$$K(x_i, x_j) = \exp(-\gamma \|x_i - x_j\|^2). \tag{9}$$

Where x_i and x_j are vectors of features computed from training or test samples in the input space. It should be noted that the accuracy of support vector machine has highly dependent on the selection of its three factors, including γ, ε and C. In order to achieving high accuracy in predictions, the PSO algorithm was employed to obtain the optimal values of these three factors.

Computational flowchart for hybrid SVM-PSO is represented in Fig. 4.

2.4. Adaptive neuro-fuzzy inference system (ANFIS)

This model was firstly presented by Jang [54] and is in fact a fuzzy Sugeno model. The most striking feature of ANFIS is its approximation and actually it is capable of approximating any real continuous function on a compact set to any degree of accuracy [55]. The other advantages of this model include facilitation of learning and adaptation of adaptive systems which is actually one of the reasons of using this model. Two

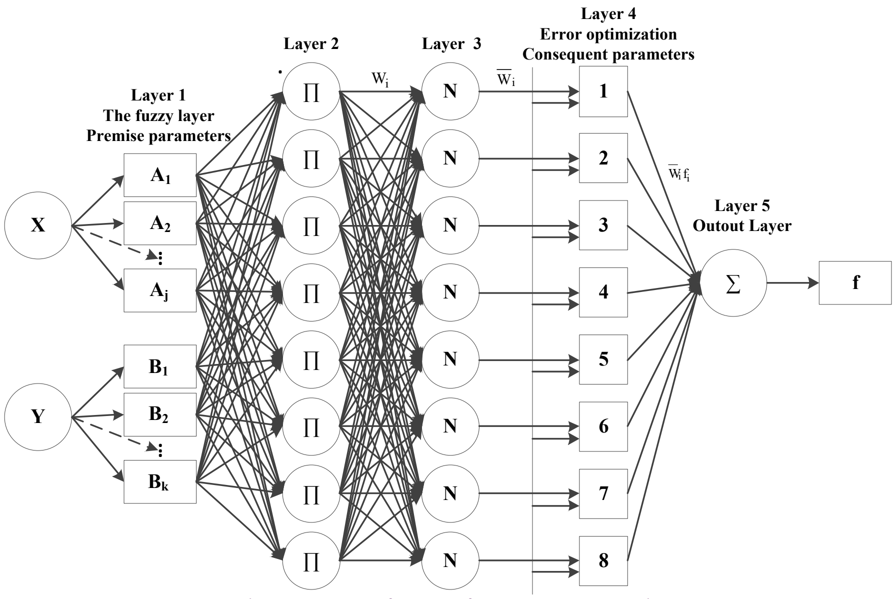

Fig. 5. Adaptive neuro fuzzy inference system architecture.

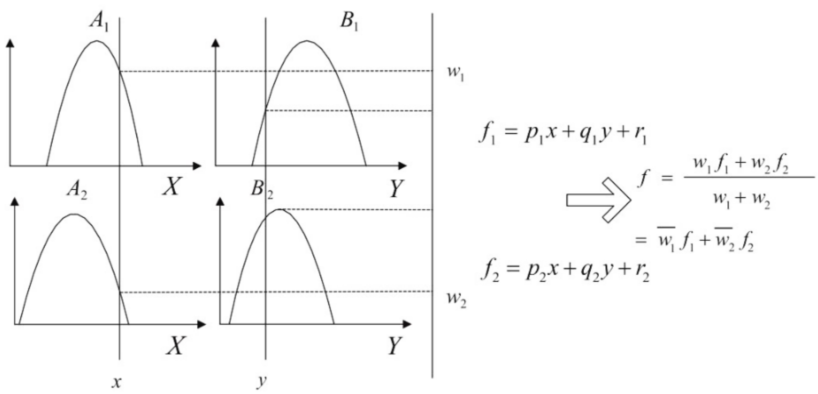

Fig. 6. First-order Takagi–Sugeno fuzzy model with two rules and two input parameters [43].

fuzzy if–then rules are considered as follow to present the ANFIS architecture. These rules are on the basis of Sugeno model's first order [56]:

$$Rule\ 1: \text{ If } x \text{ is } A_1 \text{ and } y \text{ is } B_1, \text{ then } f_1 = p_1x + q_1y + r_1. \tag{10}$$

$$Rule\ 2: \text{ If } x \text{ is } A_2 \text{ and } y \text{ is } B_2, \text{ then } f_2 = p_2x + q_2y + r_2. \tag{11}$$

where x and y are the inputs, A_i and B_i are the fuzzy sets, f_i are the outputs within the fuzzy region specified by the fuzzy rule, p_i, q_i and r_i are the design parameters that are determined during the training process . Fig. 5 shows the corresponding equivalent ANFIS architecture.

As can be seen in Fig. 5, the adaptive neuro fuzzy inference system architecture is consist of five layers which contains several nodes in each layer. The input signals of current layer are being fed by output signals from the nodes of the previous layer. In fact after manipulation by the node function in the current layer, the output will be served as input signals for the subsequent layer. Fig. 6 shows the first-order of Takagi–Sugeno fuzzy model with two rules and two input parameters.

The output of the i th node in layer l is denoted as $O_{l,i}$ and the function of nodes in a layer is similar. The output is the weighted average of the individual rule outputs and is itself a crisp value.

The first layer is known as fuzzy layer. Each node of this layer is an adaptive one with the ability of making the membership grade of a fuzzy set with the help of their Gaussian membership function.

$$O_{1,j} = \mu_{Aj}(X) = \exp\left[-\left(\frac{X - c_j}{a_j}\right)^2\right], \quad j = 1,2, \dots, m. \tag{12}$$

$$O_{1,k} = \mu_{Bk}(Y) = \exp\left[-\left(\frac{Y - c_k}{a_k}\right)^2\right], \quad k = 1,2, \dots, n. \tag{13}$$

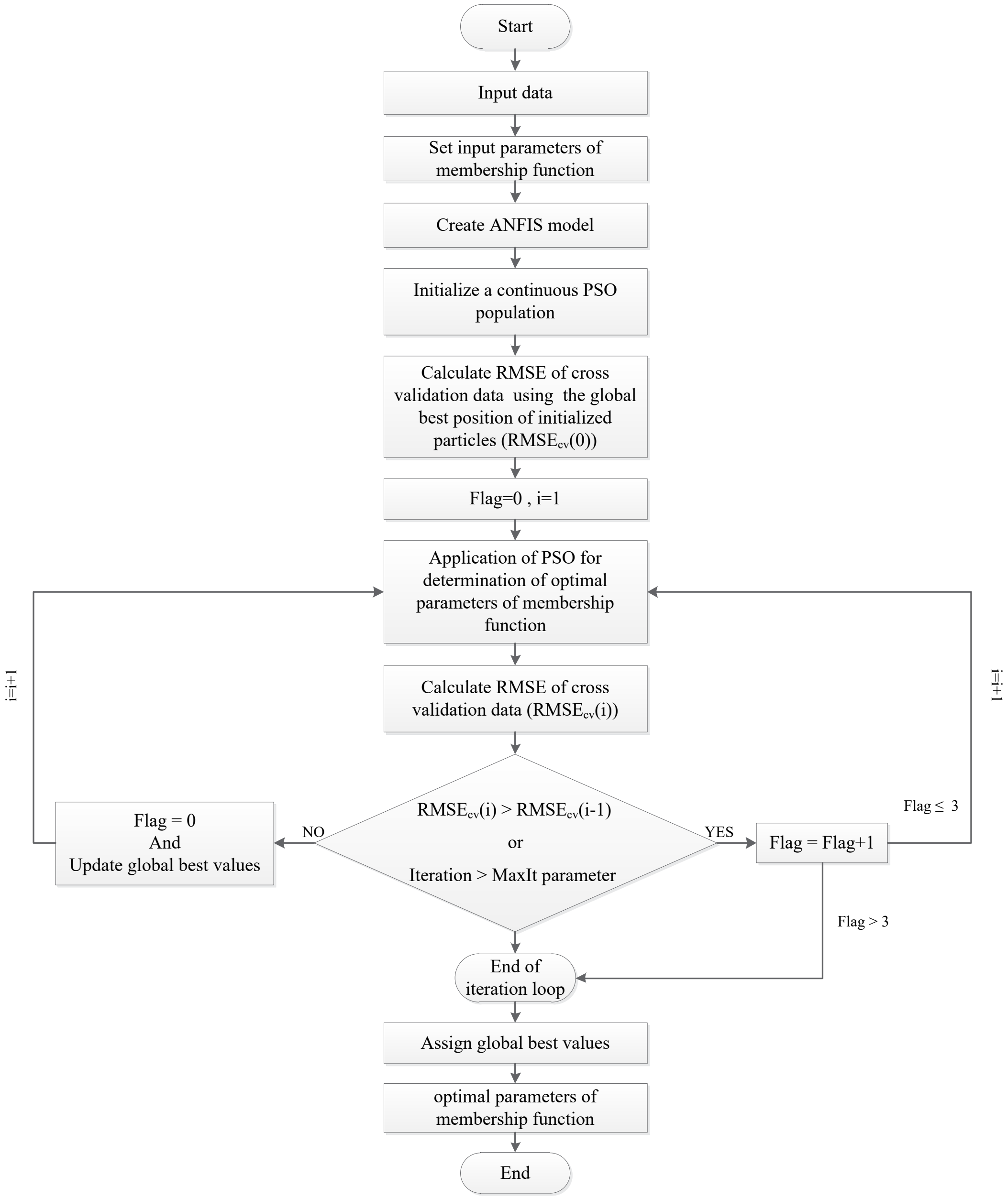

.Fig. 7. Flowchart of ANFIS-PSO

Where a_i and c_i are premise parameters. Also, X and Y are the inputs to node i and Ai and Bi are the linguistic labels associated with the node function.

Every node in layer 2 is a fixed node, marked by a circle, labeled Π, representing the firing strength of each rule, and is calculated by the fuzzy 'and' connective of 'product' of the incoming signals, that is, Π -norm operation:

$$O_{2,i} = w_i = \mu A_j(X) \times \mu B_k(Y) \tag{14}$$

The output signal w_i denotes the firing strength of the associated rule.

In layer 3, every node is a fixed node labelled N, representing the normalized firing strength of each rule. The i th node calculates the ratio of the i th rule's firing strength to the sum of the rules' firing strengths using Eq. (15):

$$O_{3,i} = \overline{w_i} = \frac{w_i}{\sum_{t=1}^{m\times n} w_t}. \tag{15}$$

The outputs of this layer are called normalized firing strengths.

Eq. (16), represents the node function of layer 4 and indicates the contribution of the i th rule towards the overall output. It should be mentioned that all the nodes in this layer are of an adaptive kind of nodes.

$$O_{4,i} = \overline{w_i} \times f_i = \overline{w_i} \times (p_i \times X + q_i \times Y + r_i) \tag{16}$$

Table 1. Data sources for compressive strength database.

Reference	Number of data	Gravel	Sand	Silty clay	Cement	Bentonit	Water	Curing time	Class of specimens	Compressive strength
[59]	12	795	699	0	230	30	330	7,28,42,90	1	1.54-5.86
[60]	24	0-926	509-1499	0	115-289	27-47	300-520	28,90	1	1.45-5.08
[61]	26	660-820	590-750	0-380	50-160	20-320	340-500	14,28,90	4	0.8-4.64
[62]	8	876-993	662-786	0	150-160	27-330	291-294	7,28	1	1.13-2.21
[19]	10	800	700	0	150-200	30-70	312-412	60,90	2	1.13-3.79
[8]	36	450	900	150	120	16-48	300	7,28,90	4	0.88-2.16
[63]	19	677-823	677-823	0	100-220	25-55	300-395	28,90	1	0.78-6.37
[64]	2	697-718	570-587	0	248-305	31	397	28	1	3.33-6.93
[65]	20	605-707	605-707	180-260	90-150	40-100	296-400	28,56,90	5	1.11-2.82
[17]	90	524-786	524-786	180-260	90-150	40-100	296-400	28,90,180,540	3,4,5	1.06-5.63
[66]	20	750	750	0	200-300	20-35	203-420	7,28	2	4.25-10.49
[20]	35	860-1060	530-730	0	110-170	20-40	198-306	7,28,90,180,360	2	1.13-5.86
[67]	45	750	750	0	150	32-48	400	7,28,90	2	0.49-1.67
[68]	16	775-875	775-875	0	72-224	36-168	162-302	7,28,90	4	1.37-10.89
This study	24	295-310	1290-1305	205-225	80-224	40-168	357-481	7,28,90	2,4	0.98-7.46

Gravel, Sand, Silty clay, Cement, Bentonit, in Kgm^{-3}
Water in Lm^{-3}
Curing time in day
Class of specimens: 1,2,...,5
Compressive strength in MPa

Where $\overline{w_i}$ is the output of layer 3 and p_i, q_i and r_i are the parameter sets. The parameters of layer 4 are known as consequent parameters. The minimization of the errors between the NF inference system outputs and desired results is the key function of these consequent parameters.

Layer 5 has a single node that is a fixed one labeled Σ , and marked by a circle. Eq. (17), calculates the incoming signals and these outputs can be indicated by this fixed node.

$$O_{5,i} = \sum_{i=1} (\overline{w_i} \times f_i) = \frac{\sum_i (\overline{w_i} \times f_i)}{\sum_i} = f. \tag{17}$$

In this study, among the different forms of Fuzzy membership functions, Gaussian membership function was selected to build the ANFIS architectureare. As researches conducted by Takagi and Sugeno (1985), the parameters of the membership functions are being adjusted by the ANFIS architectureare [56]. In this paper, ANFIS employs the PSO method due to the characteristic of being less computationally expensive for a given size of network topology. Computational flowchart for hybrid ANFIS-PSO is shown in Fig. 7.

2.5. Evaluation of models performance

In the present study, the performance of the ANN-PSO, SVM-PSO and ANFIS-PSO was evaluated according to the following statistical indicators:

(1)Root Mean Square Error (RMSE)

$$RMSE = \sqrt{\frac{1}{N}\sum_{i=1}^{N}(y_i - x_i)^2} \tag{18}$$

(2) Coefficient of determination (R^2)

$$R^2 = \left[\frac{1}{N}\frac{\sum_{i=1}^{N}(x_i - \bar{x})(y_i - \bar{y})}{\sigma_x.\sigma_y}\right]^2 \tag{19}$$

where N is the size of observations vector, x_i is the x value for observation i, y_i is the y value for prediction i, $\bar{x}$ is the mean x value, $\bar{y}$ is the mean y value, σ_x is the standard deviation of x, and σ_y is the standard deviation of y.

2.6. Dataset

After collecting data from different research sources and after taking into account the mean and standard deviation of the data, laboratory program with the aim of filling gaps in the data range, was designed. Reference, number and variation range of collected data for compressive and tensile strength

Table 2. Data sources of splitting tensile strength database.

Reference	Number of data	Gravel	Sand	Silty clay	Cement	Bentonit	Water	Curing time	Class of specimens	Splitting tensile strength
[69]	11	670-810	590-727	0-330	50-160	20-320	350-500	28	4	0.15-0.51
[63]	15	677-823	677-823	0	100-220	25-55	330-395	90	1	0.088-0.68
[70]	8	590-710	660-810	160-380	120	50	350-400	28	4	0.13-0.27
[17]	51	524-786	524-786	180-260	90-150	40-100	296-400	28,90,180	3,4	0.14-0.72
[13]	6	690-760	610-680	190-310	120-130	20-50	400-450	28	3	0.13-0.27
[68]	4	875	875	0	72-144	36-108	162-252	28,90	2	0.6-1.1
This study	12	295-310	1290-1305	205-225	80-224	40-168	357-481	28,90	2	0.06-0.47

Gravel, Sand, Silty clay, Cement, Bentonit, in Kgm^{-3}
Water in Lm^{-3}
Curing time in day
Class of specimens: 1,2,...,4
Splitting tensile strength in MPa

Table 3. Statistical characteristics of the compressive strength data set attributes.

Statistical parameter	Gravel	Sand	Silty clay	Cement	Bentonit	Water	Curing time	Class of specimens	Compressive strength
Minimum	0	509	0	50	16	162	7	1	0.49
Maximum	1060	1499	380	305.4	320	520	540	5	10.89
Mean	670.19	764.57	97.88	148.25	53.47	346.68	72.47	-	2.8
Standard deviation	185.84	181.88	101.57	45.73	31.25	62.67	101.53	-	1.95
Median	707	730	140	140	44.8	356.7	28	3	2.12

Gravel, Sand, Silty clay, Cement, Bentonit, in Kgm^{-3}
Water in Lm^{-3}
Curing time in day
Class of specimens: 1,2,...,5
Compressive strength in MPa

Table 4. Statistical characteristics of the splitting tensile strength data set attributes.

Statistical parameter	Gravel	Sand	Silty clay	Cement	Bentonit	Water	Curing time	Class of specimens	Splitting tensile strength
Minimum	295	524	0	50	20	162	28	1	0.06
Maximum	875	1305	380	224	320	500	180	4	1.1
Mean	647.7	752.93	173.64	129.53	66.82	365.74	59.5	-	0.31
Standard deviation	143.87	207.73	94.9	32.21	36.07	52.96	36.84	-	0.16
Median	666.25	670	180	120	70	370	28	3	0.27

Gravel, Sand, Silty clay, Cement, Bentonit, in Kgm^{-3}
Water in Lm^{-3}
Curing time in day
Class of specimens: 1,2,...,4
Splitting tensile strength in MPa

are given in Tables 1 and 2, respectively:

Statistical characteristics for each of data set attribute are presented in Tables 3 and 4.

The shape and dimension of each class for compressive and tensile strength are given in Tables 5 and 6, respectively.

3. APPLICATION AND RESULTS

3.1. ANN-PSO method

In this study, the ANN toolbox of MATLAB was employed to assess ANN method. The main feature of this toolbox can be attributed to allocate initial weights and biases randomly in each run. In order to train ANN, 30%, 10% and 60% of records were considered as testing, cross validating, and training set, respectively. Before running the ANN method in MATLAB, the training and testing data were normalized between 0 and 1. With the aim of preventing the negative effects of random allocation of initial weights and biases on the performance of the trained ANN, a code was developed in MATLAB. This code actually handles the trial and error process automatically to determine the optimum architecture of ANN. After the

Table 5. Classification of specimens for prediction models of compressive strength.

Specimen size	Class number
Cylinder 150×300	1
Cylinder 100×200	2
Cube 150×150×150	3
Cube 100×100×100	4
Prism 150×150×300	5

Table 6. Classification of specimens for prediction models of splitting tensile strength.

Specimens size	Class number
Cylinder 150×300	1
Cylinder 100×200	2
Cube 150×150×150	3
Cube 100×100×100	4

evaluation of neurons of hidden layer by program, the best ANN architecture with the minimum RMSE of the testing set was chosen.

A neural network with two hidden layer was used for both compressive and splitting tensile strength model with different architecture. In order to having a proper prediction accuracy 8-51-5-1 architecture for compressive strength model and 8-20-29-1 architecture for splitting tensile strength model was chosen. In these two architectures, 51 and 20 are the number of neurons in the first hidden layer and 5 and 29 are the number of neurons in the second hidden layer.

In both models the hyperbolic tangent sigmoid transfer function (tansig) in hidden layers and linear transfer function (Purelin) in output layer was used. Also the Levenberg-Marquardt algorithm [71, 72] was used to train the neural network.

Then, according to the best architecture obtained for each case, the PSO optimization algorithm was used to find the best weights and biases. Considered parameters for PSO algorithm are given in Table 7.

The performance of ANN-PSO for predicting compressive and splitting tensile strength using training and testing sets, is demonstrated in Fig.s 10 and 11, respectively. Also, the RMSE and R^2 values for each model are given in Table 8.

As can be seen in the Table 8, the coefficient of determination (R^2) between observed and predicted values of compressive strength for training and testing sets is 0.989 and 0.956, respectively. This parameter in case of the splitting tensile strength for training and testing sets is 0.999 and 0.968, respectively. In general, it is observed that ANN method can predict compressive and splitting tensile strength with R^2 more than 0.95. It is also visible that the accuracy of ANN method in prediction of splitting tensile strength is more than its accuracy in predicting of compressive strength.

3.2. SVM-PSO method

In order to train SVM-PSO, 30%, 10%, and 60% of dataset records were considered as testing, cross validating and training set, respectively. The PSO parameters for optimization of SVM parameters are given in Table 9. The optimal values of γ , ε and C by using the PSO algorithm are given in Table 10.

Fig.s 10 and 11 illustrate the performance of SVM-PSO method for predicting compressive and splitting tensile strength based on training and testing sets, respectively. Also, the RMSE and R^2 values for each model are given in Table 11.

Table 11 shows that the coefficient of determination (R^2) of predicted values for compressive strength using SVM-PSO method in case of training and testing data by is 0.996 and 0.921, respectively. This parameter in case of the splitting tensile strength for training and testing data is 0.999 and 0.936, respectively. As evidence, the accuracy of SVM-PSO method is case of training set is very high, however, due to reduced amounts of R^2 in case of testing set in comparison with training data, it can be concluded that this method has fewer generalization capability than artificial neural network. Also it is evidence that similar to ANN-PSO method, the accuracy of SVM-PSO method in prediction of splitting tensile strength is more than its accuracy in predicting of compressive strength.

3.3. ANFIS-PSO method

In the application of ANFIS-PSO method, 30%, 10%, and 60% of records were considered as testing, cross validating and training set, respectively. Optimum Architecture of ANFIS in terms of number of rules was determined by assessing different architectures using ANFIS toolbox of MATLAB and the optimum number of rules was determined as 10 in both compressive and splitting tensile strength models. ANFIS-PSO procedure was then employed to determine the optimum parameters of membership functions. Table 12 shows the PSO parameters for optimization of this method.

Fig.s 12 and 13 represent the performance of ANFIS-PSO method for predicting compressive and splitting tensile strength of training and testing set, respectively. Also, the RMSE and R^2 values for each model are given in Table 13.

Table 13 shows that the values of R^2 for prediction of compressive and tensile strength in case of training set by using ANFIS-PSO is 0.967 and 0.959, respectively. These values are much less in comparison with values obtained from ANN-PSO and SVM-PSO methods. In addition, it can also be seen that the values of R^2 for predicted value of compressive and tensile strength in case of testing set is 0.899 and 0.932, respectively that are less than values obtained using ANN-PSO and SVM-PSO methods. In general, it can be stated that ANFIS-PSO method does not have the possibility of predicting compressive strength with high accuracy.

4. COMPARISON OF ANN-PSO, SVM-PSO AND ANFIS-PSO

In Table 14, the prediction results of the compressive and tensile strength of plastic concrete for the Overall data

Table 7. PSO parameters for ANN optimization.

Parameters	Compressive strength	Splitting tensile strength
Number of particles	500	500
Number of iterations	100	100
Cognitive acceleration, C_1	1	1
Social acceleration, C_2	2	2
Initial inertia weight , ω	1	1
Inertia weight damping ratio, ω_{damp}	0.99	0.99

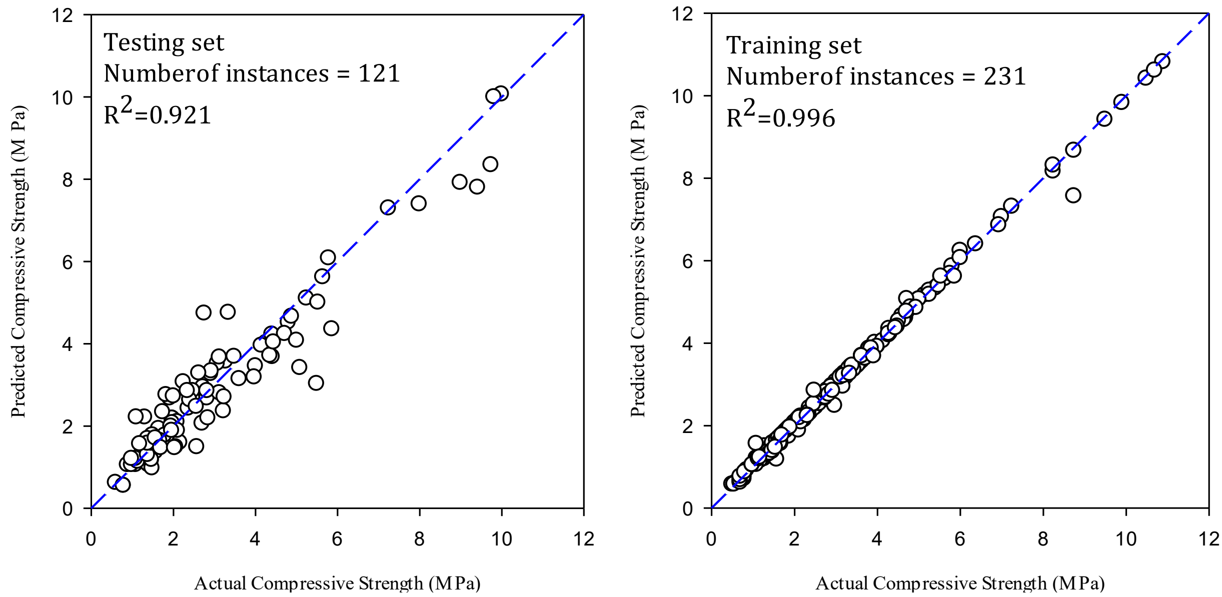

Fig. 8. Performance of ANN-PSO model for prediction of compressive strength.

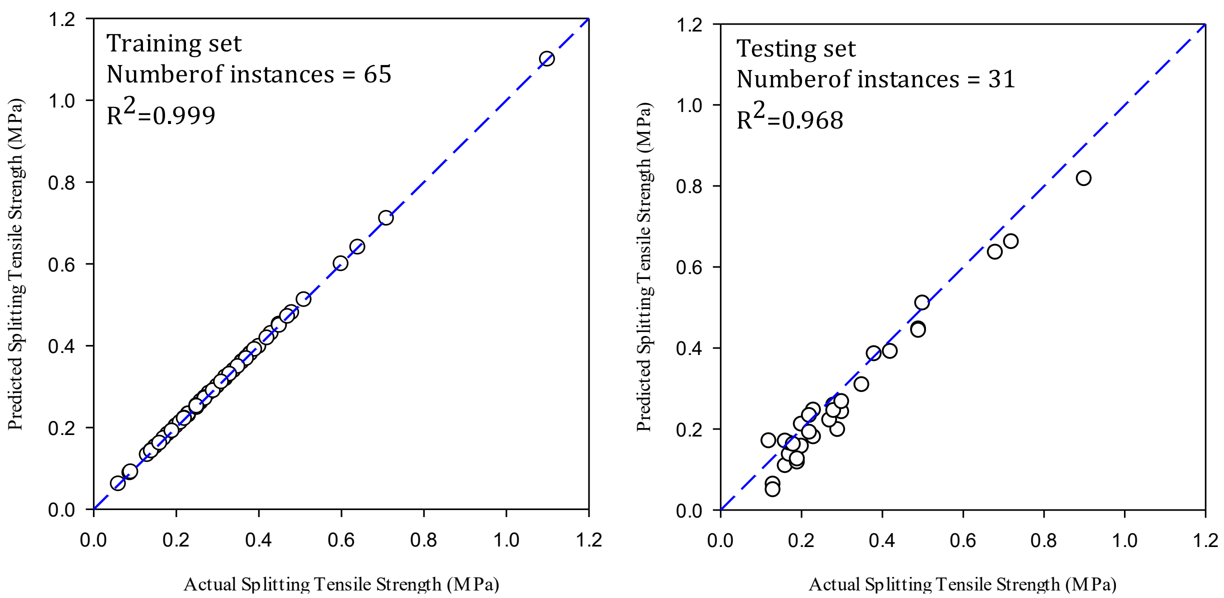

Fig. 9. Performance of ANN-PSO model for prediction of splitting tensile strength.

set by using six methods of ANN, ANN-PSO, SVM, SVM-PSO, ANFIS and ANFIS-PSO are given. As can be seen, among the evaluated methods in this paper, ANN-PSO method, compared to other methods, provides more accurate prediction of compressive and tensile strength of plastic concrete. Also, the better accuracy of SVM-PSO compared to accuracy of ANFIS-PSO is visible. In total, with respect to the assessment conducted in this paper, ANN-PSO method for predicting the compressive and tensile strength of plastic concrete is recommended and it can be expected

Table 8. The accuracy of ANN-PSO for non-normalized dataset.

Model	Training Set		Testing Set	
	R^2	RMSE (MPa)	R^2	RMSE (MPa)
Compressive strength	0.989	0.207	0.956	0.427
Splitting tensile strength	0.999	0.002	0.968	0.048

Table 9. PSO parameters for SVM optimization.

Parameters	Compressive strength	Splitting tensile strength
Number of particles	200	200
Number of iterations	100	100
Cognitive acceleration, C_1	1	1
Social acceleration, C_2	2	2
Initial inertia weight , ω	1	1
Inertia weight damping ratio, ω_{damp}	0.99	0.99

Table 10. Optimal values of γ , ε and C .

Model	γ	ε	C
Compressive strength	9.669	0.007	12.848
Splitting tensile strength	5.292	0.001	4.047

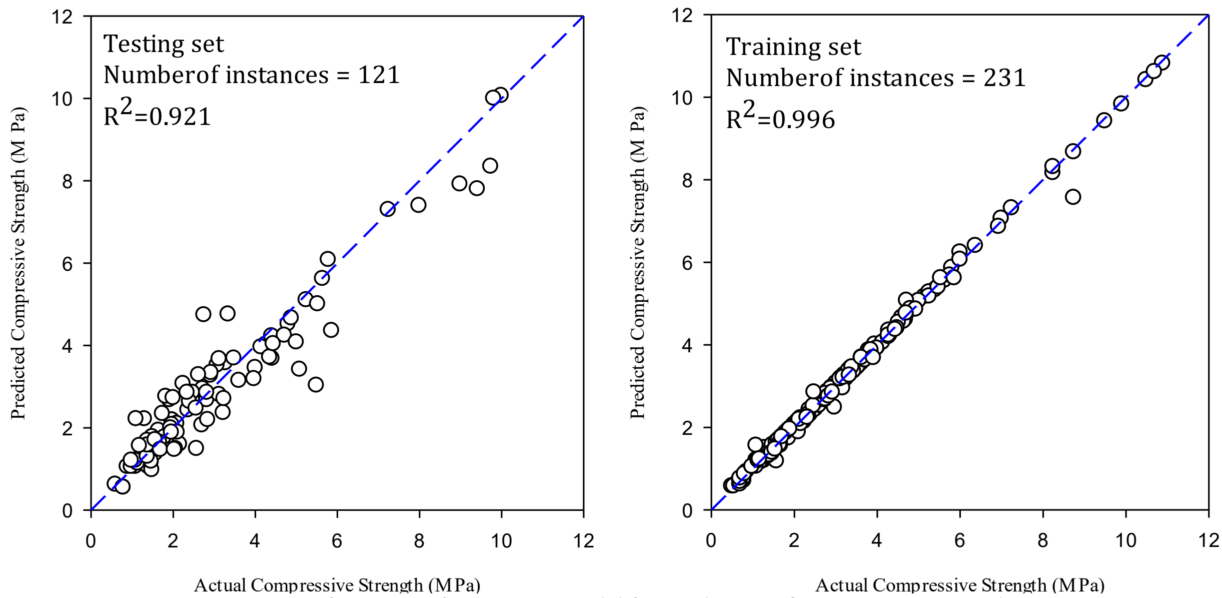

Fig. 10. Performance of SVM-PSO model for prediction of compressive strength.

that the predicted values using this method has coefficient of determination (R^2) more than 95 percent.

Fig. 14 demonstrates the predicted versus observed values of compressive strength of plastic concrete using three different hybrid machine learning methods. As can be seen, in most cases, the percentage of error in predicting compressive strength is less than 30 percent. Fig. 15 shows the predicted versus observed values of splitting tensile strength of plastic concrete using ANN-PSO, SVM-PSO, and ANFIS-PSO. It is evidence that in most cases the percentage of error in predicting splitting tensile strength is less than 20 percent.

5. SENSITIVITY ANALYSIS

In order to investigate the effect of different input parameters on the compressive and splitting tensile strength of plastic concrete, the Cosine Amplitude Method (CAM), was employed. In this method, the express similarity relation between the target values and the input parameters is used. In this method, all of

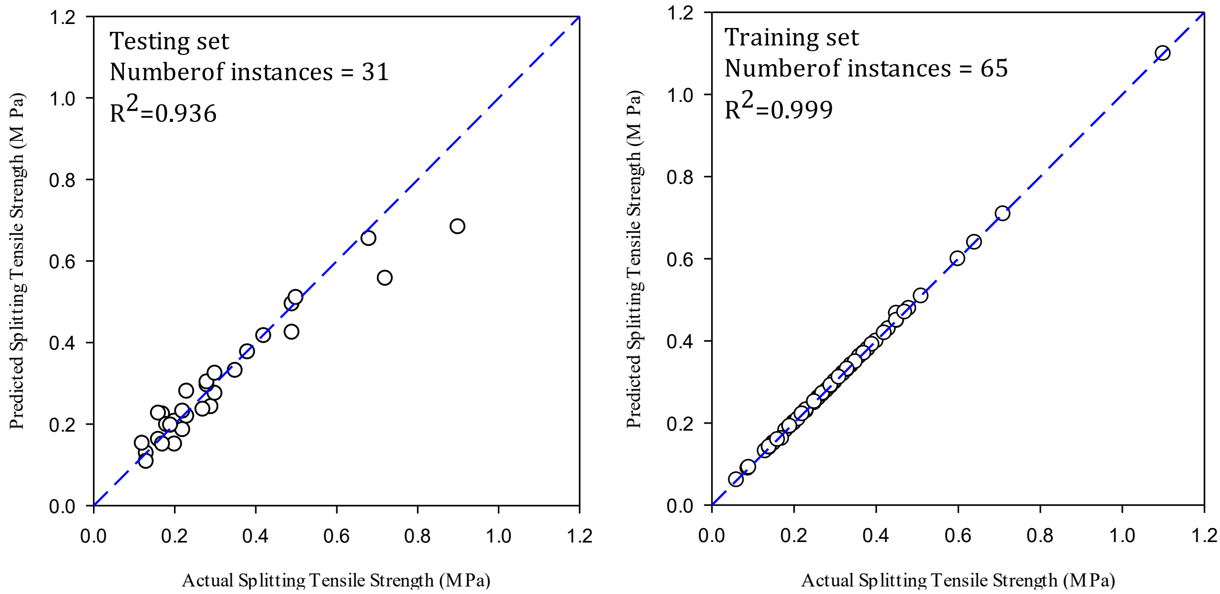

Fig. 11. Performance of SVM-PSO model for prediction of splitting tensile strength.

Table 11. The accuracy of SVM-PSO.

Model	Training Set		Testing Set	
	R^2	RMSE (MPa)	R^2	RMSE (MPa)
Compressive strength	0.996	0.124	0.921	0.577
Splitting tensile strength	0.999	0.003	0.936	0.052

Table 12. PSO parameters for ANFIS optimization.

Parameters	Compressive strength	Splitting tensile strength
Number of particles	45	40
Number of iterations	1000	500
Cognitive acceleration, C_1	1	1
Social acceleration, C_2	2	2
Initial inertia weight , ω	1	1
Inertia weight damping ratio, ω_{damp}	0.99	0.99

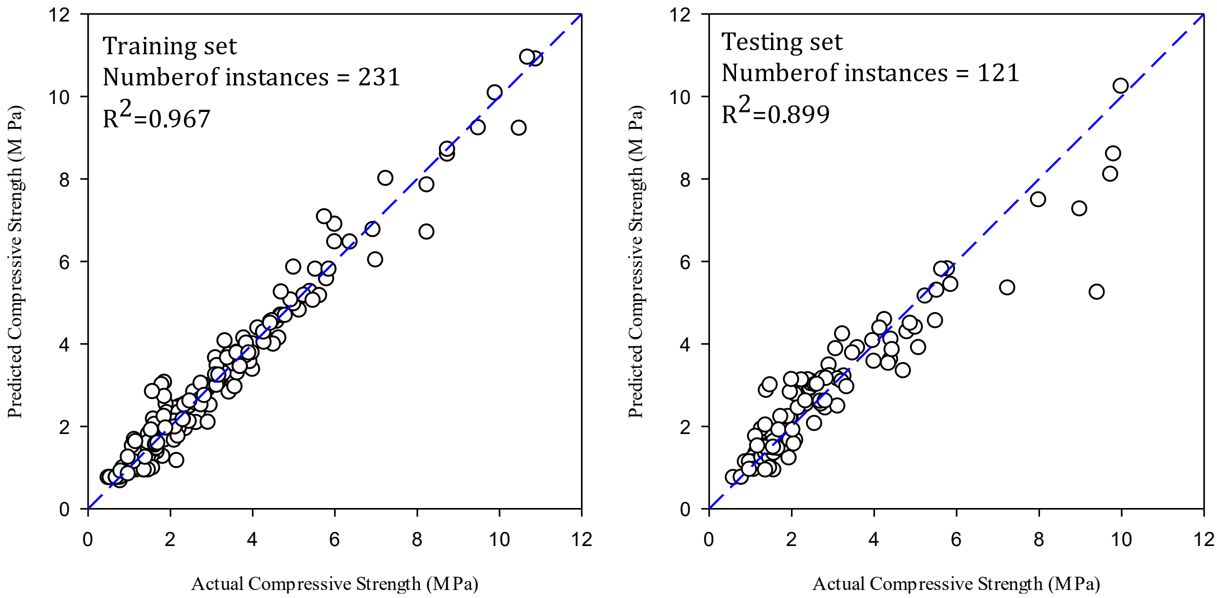

Fig. 12. Performance of ANFIS-PSO model for prediction of compressive strength.

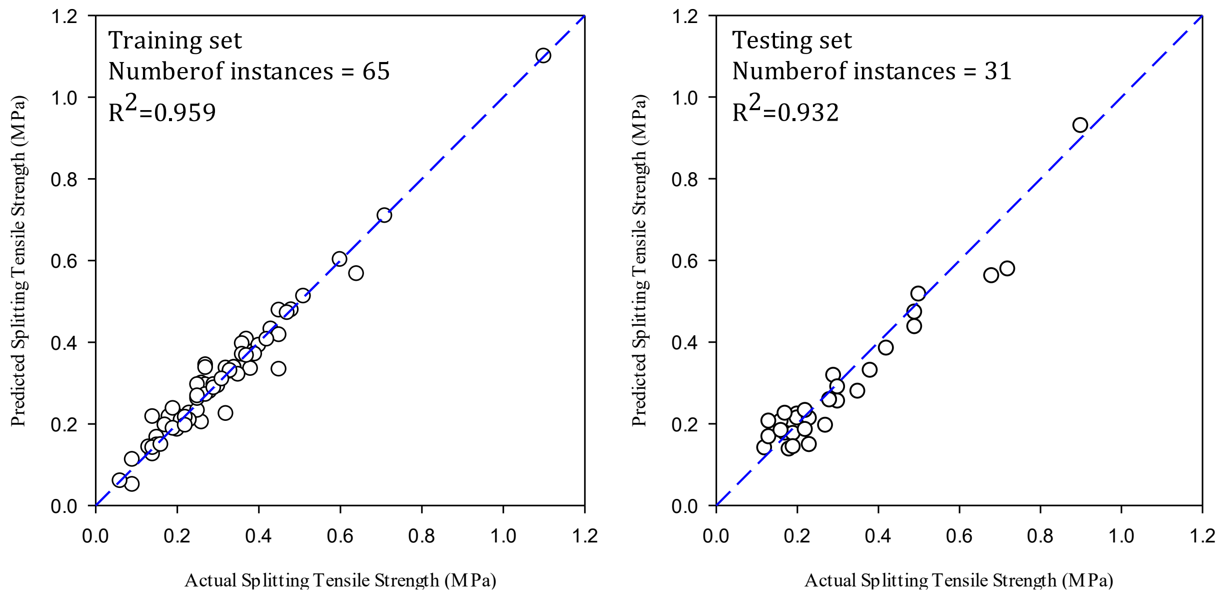

Fig. 13. Performance of ANFIS-PSO model for prediction of splitting tensile strength.

Table 13. The accuracy of ANFIS-PSO.

Model	Training Set		Testing Set	
	R^2	RMSE (MPa)	R^2	RMSE (MPa)
Compressive strength	0.967	0.354	0.899	0.669
Splitting tensile strength	0.959	0.033	0.932	0.057

Table 14. The accuracy of different machine learning techniques based on overall dataset.

Model	Overall Dataset											
	ANN		ANN-PSO		SVM		SVM-PSO		ANFIS		ANFIS-PSO	
	R^2	RMSE	R^2	RMSE	R^2	RMSE	R^2	RMSE	R^2	RMSE	R^2	RMSE
Compressive strength	0.923	0.500	0.967	0.353	0.895	0.723	0.942	0.469	0.855	0.845	0.914	0.572
Splitting tensile strength	0.950	0.037	0.971	0.031	0.901	0.053	0.960	0.034	0.891	0.060	0.941	0.040

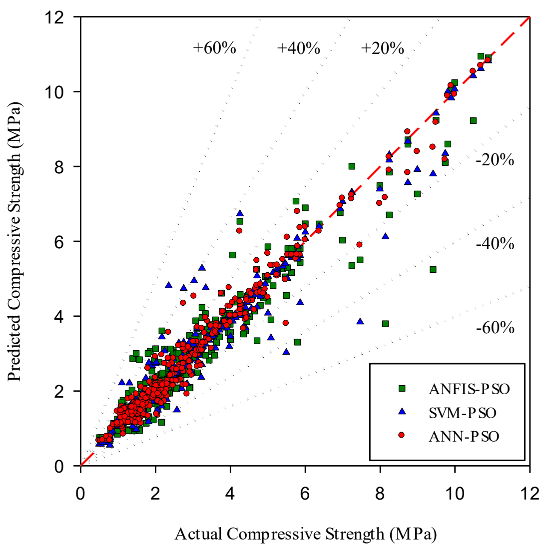

Fig. 14. Comparison of various predicted values of compressive strength for different models.

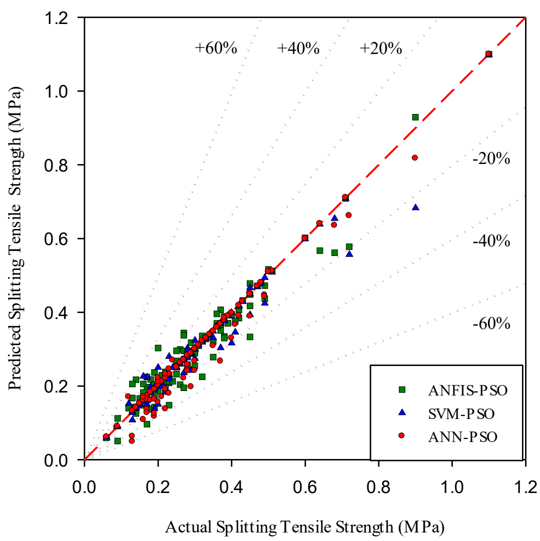

Fig. 15. Comparison of various predicted values of splitting tensile strength for different models.

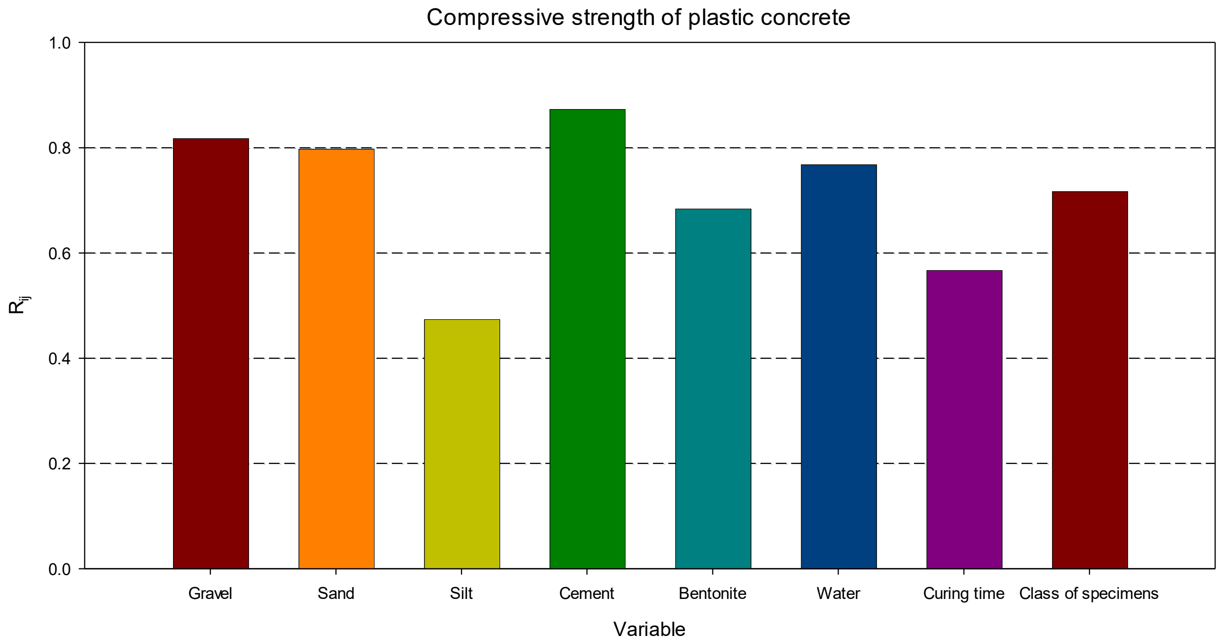

Fig. 16. Strength of the relationship between different parameters and compressive strength of plastic concrete.

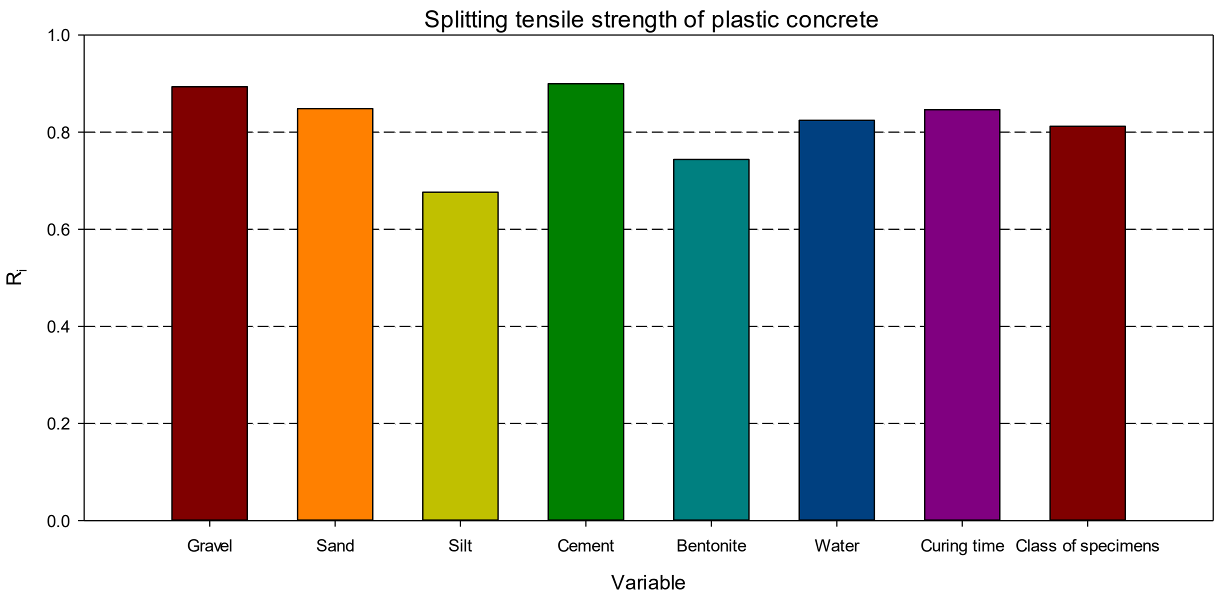

Fig. 17. Strength of the relationship between different parameters and splitting tensile strength of plastic concrete.

data pairs are expressed in the common X-space. They would form a data array X defined as Eq. (20) [73]:

$$X = \{x_1 + x_2 + x_3 + \ldots + x_n\} \tag{20}$$

Where x_i, is a vector of the length of m and is shown in the Eq. (21).

$$x_i = \{x_{i1} + x_{i2} + x_{i3} + \ldots + x_{im}\} \tag{21}$$

Thus, each record of the dataset can be assumed as a point in the m-dimensional space and this point requires m-coordinates to be fully defined. Equation (22) can be used to compute the strength of the relationship between xi and xj:

$$R_{ij} = \frac{\sum_{k=1}^{m} x_{ik} x_{jk}}{\sqrt{\sum_{k=1}^{m} x_{ik}^2 \sum_{k=1}^{m} x_{jk}^2}} \tag{22}$$

Regarding the CAM method, the strength of the relationship between compressive strength of plastic concrete and input parameters, and also splitting tensile strength of plastic concrete and input parameters were presented in Fig.s 16 and 17, respectively. The results show that cement is the most influencing factor on the compressive and splitting tensile strength of plastic concrete. Also, silty clay is the least sensitive parameter.

6. CONCLUSIONS

In this paper, three hybrid machine learning methods including ANN, SVM and ANFIS optimized with PSO were employed to predict the compressive as well as splitting tensile strength of plastic concrete. In these models, input data were considered as gravel (5-19 mm) in kg/m^3, sand (0-5 mm) in kg/m^3, silty clay (particles smaller than 0.075 mm) in kg/m^3, cement in kg/m^3, bentonite in kg/m^3, water in l/m^3, curing time in days and class of shape and size of specimens (5 classes for compressive strength and 4 classes for splitting tensile strength). The following conclusions can be drawn from this study.

1. The optimum architecture of ANN for predicting compressive and splitting tensile strength of plastic concrete is 8-51-5-1 and 8-20-29-1, respectively. In these two architectures, 51 and 20 are the number of neurons in the first hidden layer and 5 and 29 are the number of neurons in the second hidden layer.

2. Coefficient of determination (R^2) between observed and predicted values of compressive strength using ANN-PSO, SVM-PSO and ANFIS-PSO methods in case of training set was obtained as 0.989, 0.996, and 0.967, respectively. This value for testing set was obtained as 0.976, 0.921 and 0.899 using ANN-PSO, SVM-PSO and ANFIS-PSO, respectively.

3. Coefficient of determination (R^2) between observed and predicted values of splitting tensile strength using ANN-PSO, SVM-PSO and ANFIS-PSO methods in case of training set was obtained as 0.999, 0.999, and 0. 957, respectively. This value for testing set was obtained as 0.968, 0.936 and 0.932 using ANN-PSO, SVM-PSO and ANFIS-PSO, respectively.

4. Application of ANN-PSO is superior to SVM-PSO and ANFIS-PSO for predicting compressive and tensile strength of plastic concretes.

5.Developed ANN-PSO can be used to predict compressive strength as well as splitting tensile strength of plastic concrete with respect to constituent materials and geometry of plastic concrete specimen without any need of conducting experimental tests.

6. The results of parametric analysis show that the cement is the most influencing factor on the compressive and splitting tensile strength of plastic concrete, while, silty clay is the least sensitive parameter.

CONFLICT OF INTERESTS

The authors declare that there is no conflict of interests regarding the publication of this paper.

REFERENCES

[1] T.W. Kahl, J.L. Kauschinger, E.B. Perry, Repair, Evaluation, Maintenance, and Rehabilitation Research Program: Plastic Concrete Cutoff Walls for Earth Dams, DTIC Document, 1991.

[2] L.M. Hu, D.Y. Gao, Y.Z. Li, S.Q. Song, Analysis of the Influence of Long Curing Age on the Compressive Strength of Plastic Concrete, in: Advanced Materials Research, Trans Tech Publ, 2012, pp. 200-203.

[3] ICOLD, Filling materials for watertight cut off walls. Bulletin, in, International Committee of Large Dams, Paris, France, 1995.

[4] S.L. Garvin, C.S. Hayles, The chemical compatibility of cement–bentonite cut-off wall material, Construction and Building Materials, 13(6) (1999) 329-341.

[5] D. Koch, Bentonites as a basic material for technical base liners and site encapsulation cut-off walls, Applied Clay Science, 21(1) (2002) 1-11.

[6] M. Naderi, Effect of different constituent materials on the properties of plastic concrete, International Journal of Civil Engineering, 3(1) (2005) 10-19.

[7] D.Y. Gao, K. Yan, L.M. Hu, S.Q. Song, Influence of bentonite types on the properties of plastic concrete Journal of Hydroelectric Engineering, 28(3) (2009) 112-116.

[8] A. Tahershamsi, A. Bakhtiyari, N. Binazadeh, Effects of clay mineral type and content on compressive strength of plastic concrete (In Persian), Iranian Journal of Mining Engineering, 4(7) (2009) 35-42.

[9] G.Q. Ding, L.H. Jiang, H.Q. Chu, Q. Zhu, Influences of types and dosage of bentonite on properties of plastic concrete, Advances in Science and Technology of Water Resources, 31(2) (2011) 34-37.

[10] A. Pashazadeh, M. Chekani Azar, Estimating an Appropriate Plastic Concrete Mixing Design for Cutoff Walls to Control Leakage under the Earth Dam, Journal of Basic and Applied Scientific Research, 1(9) (2011) 1295-1299.

[11] A.A. Ata, T.N. Salem, N.M. Elkhawas, Properties of soil–bentonite–cement bypass mixture for cutoff walls, Construction and Building Materials, 93 (2015) 950-956.

[12] J.L. García-Siñeriz, M.V. Villar, M. Rey, B. Palacios, Engineered barrier of bentonite pellets and compacted blocks: State after reaching saturation, Engineering Geology, 192 (2015) 33-45.

[13] P. Zhang, Q.Y. Guan, Q.F. Li, Mechanical Properties of Plastic Concrete Containing Bentonite, Research Journal of Applied Sciences, Engineering and Technology, 5(4) (2013) 1317-1322.

[14] Y. Yu, J. Pu, K. Ugai, Study of mechanical properties of soil-cement mixture for a cut-off wall, Soils Found, 37(4) (1997) 93-103.

[15] H. Abbaslou, A.R. Ghanizadeh, A.T. Amlashi, The compatibility of bentonite/sepiolite plastic concrete cut-off wall material, Construction and Building Materials, 124 (2016) 1165-1173.

[16] S. Hinchberger, J. Weck, T. Newson, Mechanical and hydraulic characterization of plastic concrete for seepage cut-off walls, Canadian Geotechnical Journal, 47(4) (2010) 461-471.

[17] L.M. Hu, stress-strain relation model and failure criterion of plastic concrete under compression (In Chinese), Material processing engineering school of materials science and engineering, Zhengzhou, China, 2012.

[18] A. Mahboubi, A. Ajorloo, Experimental study of the mechanical behavior of plastic concrete in triaxial compression, Cement and concrete research, 35(2) (2005) 412-419.

[19] A. Mahboubi, M. Anari, Effects of Mixing Proportions and Sample Age on Mechanical Properties of Plastic Concrete; An Experimental Study, in: First international conference on concrete technology, Tabriz, Iran, 2009.

[20] Y.P. Pisheh, S.M.M. Hosseini, Stress-strain behavior of plastic concrete using monotonic triaxial compression tests, Journal of Central South University, 19(4) (2012) 1125-1131.

[21] J.S. Chou, C.K. Chiu, M. Farfoura, I. Al-Taharwa, Optimizing the prediction accuracy of concrete compressive strength based on a comparison of data-mining techniques, Journal of Computing in Civil Engineering, 25(3) (2010) 242-253.

[22] F.F. Martins, A. Camões, Prediction of compressive strength of concrete containing fly ash using data mining techniques, (2013).

[23] M. Ebrahimi, A.A. Niknafs, Increasing Cement Strength Using Data Mining Techniques, in: International Conference Data Mining, Civil and Mechanical Engineering (ICDMCME), Bali (Indonesia), 2015

[24] N.N. Eldin, A.B. Senouci, Measurement and prediction of the strength of rubberized concrete, Cement and Concrete Composites, 16(4) (1994) 287-298.

[25] M.H. Fazel Zarandi, I.B. Türksen, J. Sobhani, A.A. Ramezanianpour, Fuzzy polynomial neural networks for approximation of the compressive strength of concrete, Applied Soft Computing, 8(1) (2008) 488-498.

[26] D.K. Kim, J.J. Lee, J.H. Lee, S.K. Chang, Application of Probabilistic Neural Networks for Prediction of Concrete Strength, Journal of Materials in Civil Engineering, 17(3) (2005) 353-362.

[27] J.J. Lee, D. Kim, S.K. Chang, C.F.M. Nocete, An improved application

technique of the adaptive probabilistic neural network for predicting concrete strength, Computational Materials Science, 44(3) (2009) 988-998.

[28] R. Madandoust, R. Ghavidel, N. Nariman Zadeh, Evolutionary design of generalized GMDH-type neural network for prediction of concrete compressive strength using UPV, Computational Materials Science, 49(3) (2010) 556-567.

[29] R. Madandoust, J.H. Bungey, R. Ghavidel, Prediction of the concrete compressive strength by means of core testing using GMDH-type neural network and ANFIS models, Computational Materials Science, 51(1) (2012) 261-272.

[30] J. Kasperkiewicz, J. Racz, A. Dubrawsk, HPC Strength Prediction Using Artificial Neural Network, Journal of Computing in Civil Engineering, 9(4) (1995) 279-284.

[31] İ.B. Topçu, M. Sarıdemir, Prediction of properties of waste AAC aggregate concrete using artificial neural network, Computational Materials Science, 41(1) (2007) 117-125.

[32] S. Subaşı, Prediction of mechanical properties of cement containing class C fly ash by using artificial neural network and regression technique, Sci Res Essay, 4(4) (2009) 289-297.

[33] S.J.S. Hakim, J. Noorzaei, M. Jaafar, M. Jameel, M. Mohammadhassani, Application of artificial neural networks to predict compressive strength of high strength concrete, Int. J. Phys. Sci, 6(5) (2011) 975-981.

[34] A. Nazari, H. Hajiallahyari, A. Rahimi, H. Khanmohammadi, M. Amini, Prediction compressive strength of Portland cement-based geopolymers by artificial neural networks, Neural Comput & Applic, (2012) 1-9.

[35] S. Kostić, D. Vasović, Prediction model for compressive strength of basic concrete mixture using artificial neural networks, Neural Comput & Applic, 26(5) (2015) 1005-1024.

[36] J.F. Moretti, C.R. Minussi, J.L. Akasaki, C.F. Fioriti, J.L.P. Melges, M.M. Tashima, Prediction of modulus of elasticity and compressive strength of concrete specimens by means of artificial neural networks, Acta Scientiarum. Technology, 38(1) (2016) 65-70.

[37] A. Sadrmomtazi, J. Sobhani, M. Mirgozar, Modeling compressive strength of EPS lightweight concrete using regression, neural network and ANFIS, Construction and Building Materials, 42 (2013) 205-216.

[38] J. Sobhani, M. Khanzadi, A. Movahedian, Support vector machine for prediction of the compressive strength of no-slump concrete, Computers and Concrete, 11(4) (2013) 337-350.

[39] S. Tesfamariam, H. Najjaran, Adaptive network–fuzzy inferencing to estimate concrete strength using mix design, Journal of materials in civil engineering, 19(7) (2007) 550-560.

[40] M.Y. Cheng, J.S. Chou, A.F. Roy, Y.W. Wu, High-performance concrete compressive strength prediction using time-weighted evolutionary fuzzy support vector machines inference model, Automation in Construction, 28 (2012) 106-115.

[41] S. Motamedi, S. Shamshirband, D. Petković, R. Hashim, Application of adaptive neuro-fuzzy technique to predict the unconfined compressive strength of PFA-sand-cement mixture, Powder Technology, 278 (2015) 278-285.

[42] S.S. Gilan, H.B. Jovein, A.A. Ramezanianpour, Hybrid support vector regression–Particle swarm optimization for prediction of compressive strength and RCPT of concretes containing metakaolin, Construction and Building Materials, 34 (2012) 321-329.

[43] Z. Yuan, L.N. Wang, X. Ji, Prediction of concrete compressive strength: Research on hybrid models genetic based algorithms and ANFIS, Advances in Engineering Software, 67 (2014) 156-163.

[44] A. Nazari, J.G. Sanjayan, Modelling of compressive strength of geopolymer paste, mortar and concrete by optimized support vector machine, Ceramics International, 41(9, Part B) (2015) 12164-12177.

[45] M. Nikoo, F. Torabian Moghadam, Ł. Sadowski, Prediction of concrete compressive strength by evolutionary artificial neural networks, Advances in Materials Science and Engineering, 2015 (2015).

[46] Y. Ayaz, A.F. Kocamaz, M.B. Karakoç, Modeling of compressive strength and UPV of high-volume mineral-admixtured concrete using rule-based M5 rule and tree model M5P classifiers, Construction and Building Materials, 94 (2015) 235-240.

[47] J. Kennedy, R.C. Eberhart, Particle swarm optimization, in: In: Proceedings of IEEE international conference on neural networks, 1995, pp. 1942–1948.

[48] S.S. Haykin, Neural networks: a comprehensive foundation, Tsinghua University Press, 2001.

[49] J.A. Freeman, D.M. Skapura, Neural Networks: Algorithms, Applications and Programming Techniques, Addison-Wesley Publishing Company, 1992.

[50] D.E. Rumelhart, G.E. Hintont, R.J. Williams, Learning representations by back-propagating errors Nature, 323 (1986) 533-536.

[51] P. Werbos, Beyond regression: new tools for prediction and analysis in the behavioral sciences, Harvard University, Cambridge, 1974.

[52] V. Vapnik, S.E. Golowich, A. Smola, Support vector method for function approximation, regression estimation, and signal processing, Advances in neural information processing systems, (1997) 281-287.

[53] V.N. Vapnik, V. Vapnik, Statistical learning theory, Wiley New York, 1998.

[54] J.S.R. Jang, ANFIS: adaptive-network-based fuzzy inference system, IEEE transactions on systems, man, and cybernetics, 23(3) (1993) 665-685.

[55] J.S.R. Jang, C.T. Sun, E. Mizutani, Neuro-fuzzy and soft computing; a computational approach to learning and machine intelligence, (1997).

[56] T. Takagi, M. Sugeno, Fuzzy identification of systems and its applications to modeling and control, IEEE transactions on systems, man, and cybernetics, (1) (1985) 116-132.

[57] D.M. Moore, R.C. Reynolds, X-ray Diffraction and the Identification and Analysis of Clay Minerals, Oxford university press Oxford, 1989.

[58] ICOLD, Soil-Cement, in, International Committee of Large Dams, Paris, France, 1986.

[59] M. Fathinaz, Assessment the effect of bentonite and soil lateral pressure on the stress-strain behavior of plastic concrete cut-off walls (In Persian), Faculty of Civil and Environmental Engineering, Amirkabir University of Technology, Tehran, Iran, 1998.

[60] A. Bagheri, M. Abdi, M. Mombeyni, Increasing the formability of plastic concrete without reducing strength by optimizing the volume of bentonite and cement slurry in the mix (In Persian), in: 6th international conference of civil engineering, Isfahan University of Technology, Isfahan, Iran, 2003.

[61] Q.F. Li, P. Zhang, Experimental research on strength of plastic concrete (In Chinese), concrete, (5) (2006) 75-79.

[62] M. Shahbaznia, M. Shokrchizadeh, Mix design of plastic concrete cutoff wall of Reservoir Dam Project in Duiraj city, in: 2nd National Conference of Dam and Hydropower Plants, Iran Water Resources and Power Development Company, Tehran, Iran, 2008.

[63] A. Ajam, R. Mohajeri Borjghaleh, Evaluation the effect of water-cement ratio on the plastic concrete cutoff walls using in dams (In Persian), in: First national conference of structure-earthquake-geotechnic, 2010.

[64] B. Hamdollah, M. Khanmohammadi, Experimental study on the possibility of using plastic concretes containing silica fume in structural members, in: 2nd National Conference of Concrete, Tehran, Iran, 2010.

[65] S.Q. Song, D.Y. Gao, K. Yan, L.M. Hu, Influece of the cementitious materials on the strength of plastic concrete, Concrete, (6) (2010) 86-88.

[66] S.H. Mousavi, H.S. Kazran, M.F. Maghrebi, The use of plastic concrete with specified aggregate in the implementation of concrete lining (In Persian), in: First national conference on civil engineering, Zibakenar, Iran, 2012.

[67] E. Dabir, Experimental evaluation of the effect of bentonite on the compressive strength, modulus of elasticity and permeability of plastic concrete (In Persian), in: 15th national conference of civil engineering students, University of Urmia, Urmia, Iran, 2014.

[68] S. Azemi, Plastic concrete cutoff walls in earth dams: a perspective of arid environment clay mineral resources, Faculty of Civil Engineering, Sirjan Univesity of Technology, Sirjan, Iran, 2015.

[69] P. Zhang, Q.F. Li, Experimental Research on Tensile Strength of Plastic Concrete, Water Power, (2) (2008) 64-66.

[70] Q.Y. Guan, P. Zhang, Effect of Clay Dosage on Mechanical Properties of Plastic Concrete, in: Advanced Materials Research, Trans Tech Publ, 2011, pp. 664-667.

[71] K. Levenberg, A method for the solution of certain non-linear problems in least squares, Quarterly of applied mathematics, 2(2) (1944) 164-168.
[72] D.W. Marquardt, An algorithm for least-squares estimation of nonlinear parameters, Journal of the society for Industrial and Applied Mathematics, 11(2) (1963) 431-441.
[73] Y. Yang, Q. Zhang, A hierarchical analysis for rock engineering using artificial neural networks, Rock Mechanics and Rock Engineering, 30(4) (1997) 207-222.

HOW TO CITE THIS ARTICLE

A. Tavana Amlashi , A.R. Ghanizadeh, H. Abbaslou, P. Alidoust, Developing three hybrid machine learning algorithms for predicting the mechanical properties of plastic concrete samples with different geometries, AUT J. Civil Eng., 4(1) (2020) 37-54.

DOI: 10.22060/ajce.2019.15026.5517